ORIGINAL PAPER

EVALUATION OF THE FLOW INDUCED BY DIFFERENT SHROUDS GEOMETRIES

PAUL ALEXANDRU DANCA[1,2], FLORENTINA BUNEA[1], FLORIN BODE[2,3], SERGIU NICOLAE[1]

Manuscript received: 12.10.2022; Accepted paper: 22.12.2022;
Published online: 30.03.2023.

Abstract. *Energy consumption continues to rise due to the increase in the quality of human life. On the other hand, production of these energies must be done with the smaller impact on the environment as possible. All these facts are challenging engineers and researchers from this domain to develop new equipments or to improve the efficiency of the energy production equipments. It was proved that in the case of turbine, if a shroud is applied, the efficiency is raised. Given that in this paper is presented a study performed on different geometry of shrouds with different fixing elements. Computational fluid dynamics (CFD) simulations were performed using ANSYS Fluent software. The numerical domain rigorously reproduces an experimental set-up from the laboratory. The rectangular fixing element do not deliver the expected result, instead it decreases the velocity in interest zone. The most important finding is that the velocity of the fluid increases by more than 50% in the most constrained section with convergent-divergent shroud.*

Keywords: *turbine shroud; kinetic energy; renewable energy; particle image velocimetry; computation fluid dynamics.*

1. INTRODUCTION

Hydropower represents one of the renewable energy resources, generated naturally and continuously. The need to build micro power plants is not only an inevitable requirement of society's development but also a possibility to achieve sustainable development, contributing to energy independence.

Run-of-river plants use the available flow of the watercourse, without storage, or with reduced storage, with the potential to produce smaller amounts of electricity for isolated locations. Improving the efficiency of hydrokinetic turbines is essential to make this technology more widespread and cost-effective.

The shrouds have the role of reducing the pressure at the exit of the turbine and therefore accelerating the water flow through the turbine. Gish and Hawbaker [1] studies two different shroud designs and their performance is compared to that of a turbine without intubation. Both shrouds had the same diffuser angle (20°) but different area ratios, cross-sectional shapes, and tip gaps.

Several numerical studies modelling the turbine as an impulse source have shown a significant improvement in power output by using a shroud [2-4] presents the performance of shrouded hydrokinetic turbines considering the effect of a central hub. The configuration

[1] National Institute for Research and Development in Electric Engineering, Department of Renewable Energy Sources and Energy Efficiency, 030138 Bucharest, Romania. E-mail: paul.danca@icpe-ca.ro
[2] Technical University of Civil Engineering of Bucharest, CAMBI Research Center, 021414 Bucharest, Romania.
[3] Technical University of Cluj Napoca, Department of Mechanical Engineering, 400114 Cluj Napoca, Romania.

shroud proposed by C. Cardona-Mancilla et al [5] consists of an augmented diffuser which shows a 71% increase in the power coefficient compared to the turbine without intubation, which has an efficiency of 82%.

The main purpose of this study is to compare the numerical results obtained with validated numerical models of two different shroud designs, in order to choose one of which will be further installed on a turbine rotor. The findings from this paper are useful in a larger research project which has the purpose to achieve a new hydrokinetic turbine.

All the boundary conditions used in the numerical model were previously obtained from experimental measurements, the results of these measurements being available already in the literature [6-9].

2. NUMERICAL STUDY

The aim of this study is to compare numerical results for different four chases (geometries of shrouds with different fixing elements) obtained through CFD simulation in Fluent software. The difference between the four cases are geometries of the fixing elements between hub and shroud (oval and rectangular) and the shroud section geometries (NACA 6412 hydrofoil and custom design featuring a convergent-divergent profile):

- case 1 – profile of shroud NACA and oval fixing element;
- case 2 – profile of shroud NACA and rectangular fixing element;
- case 3 – convergent-divergent profile of shroud and oval fixing elements;
- case 4 – convergent-divergent profile of shroud and rectangular fixing elements.

The study of two different geometries of fixing elements came from the desire to install a second contra-rotating turbine downstream of the first. The rectangular fixing element which has a 25° angle from the shroud axis, should guide the fluid flow to the second rotor. The oval fixing element is the most commonly used due to its hydrodynamic geometry. For each case were considered three fixing elements disposed at 120°. The dimensions of the two fixing elements can be seen in Figure 1.

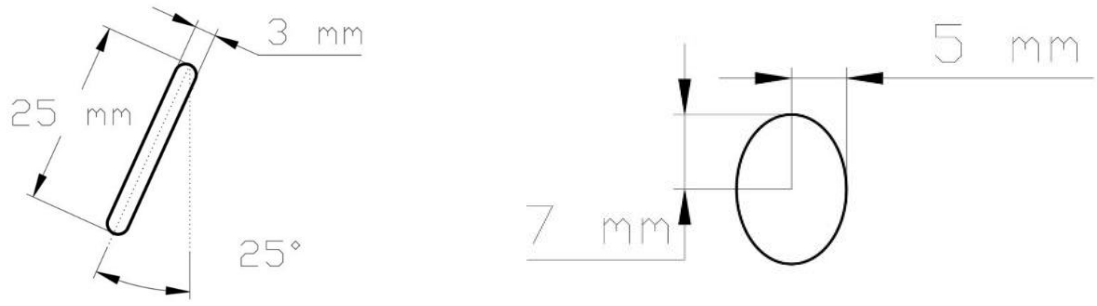

a) **b)**

Figure 1. Geometry details of a) rectangular and b) oval fixing elements

Regarding the profile geometry of the two shrouds, these are also very different because for one of the shrouds we choose NACA 6142 hydrofoil and for the other, we created a convergent-divergent profile. The length of the string, the depth and the β angle are different from one shroud to another because we wanted to maintain the same diameter at the inlet and at the outlet of the shrouds. The geometrical details of the two shrouds are presented in Figure 2.

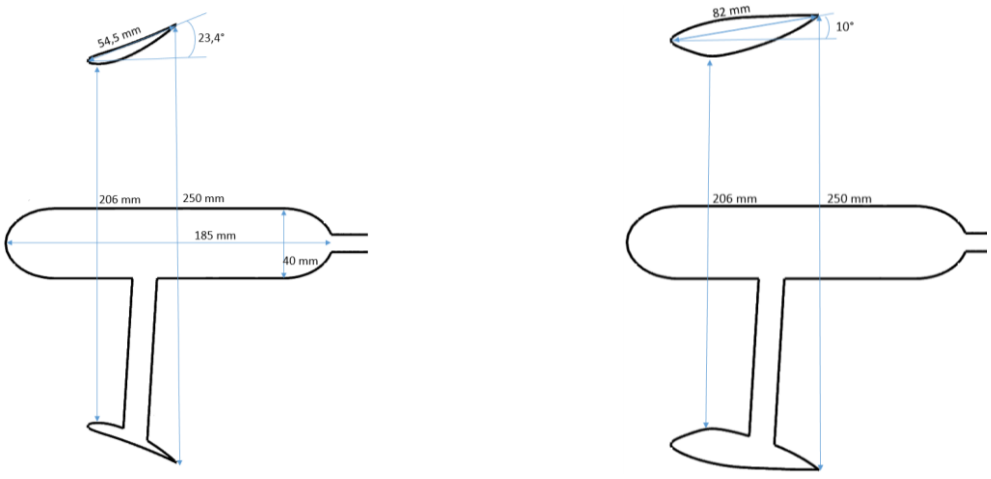

Figure 2. Geometry profile details of a) NACA and b) convergent-divergent shrouds

The hub drowns in the middle of the shroud has 185 mm in length and 40 mm in thickness. Behind the hub, there is a rod that supported the shroud during the experimental measurements. The hub nozzle has a rounded shape to provide a better flow hydrodynamics. The geometries of the four studied cases are in Figure 3.

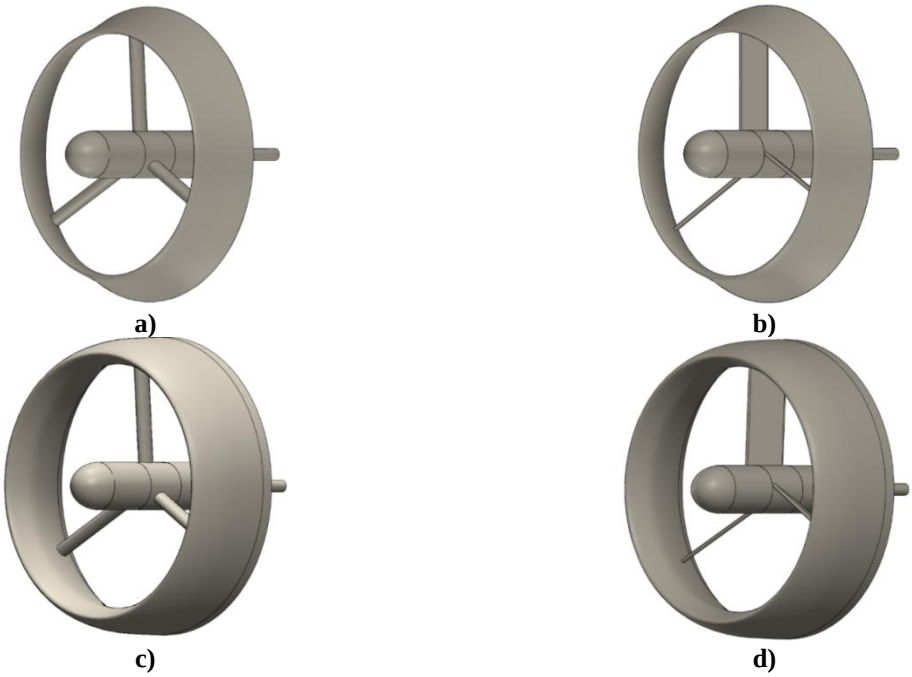

Figure 3. Geometry of the studied shrouds with the fixing elements a) case 1, b) case 2, c) case 3, d) case 4

The geometries were drawn in SolidWorks software and exported in design modeller to create the mesh. As we have 4 cases to study and each have a different geometry, 4 meshes were generated, each having around 10 million elements. The mesh grid had 8 boundary layers. The numerical grid was generated in two separate stages. First, a mesh was created using Ansys Meshing, consisting of ~9 million tetrahedral elements and after that, the numerical grid was converted to hexahedral elements in ANSYS Fluent software (Fig. 4). The final numerical grids have around ~1.3 million hexahedral elements for all the analysed cases. We adopted this strategy due to the fact that polyhedral cells mesh has more advantages than a tetrahedral one. Some of these advantages are: reduced numerical diffusion, the gradients are approximated better, are less sensitive to stretching than tetrahedral [10, 11]. For the near-

wall modelling, the standard wall function was used. The non-dimensional wall distance y+ was computed and it has the maximum value of 40.1 for the case 1, which corresponds to a desired y+ value according to the literature [12]. The maximum values of y+ were close to this value for the other cases. The turbulence model used for the numerical simulation was RNG k-ε. For the pressure-velocity coupling we utilized the COUPLED algorithm. CFD 3D simulations were performed in Fluent 2020 R2 software. In Figure 4 are presented planes extracted in median plane of the computational domain, with the discretization mesh created for each studied case.

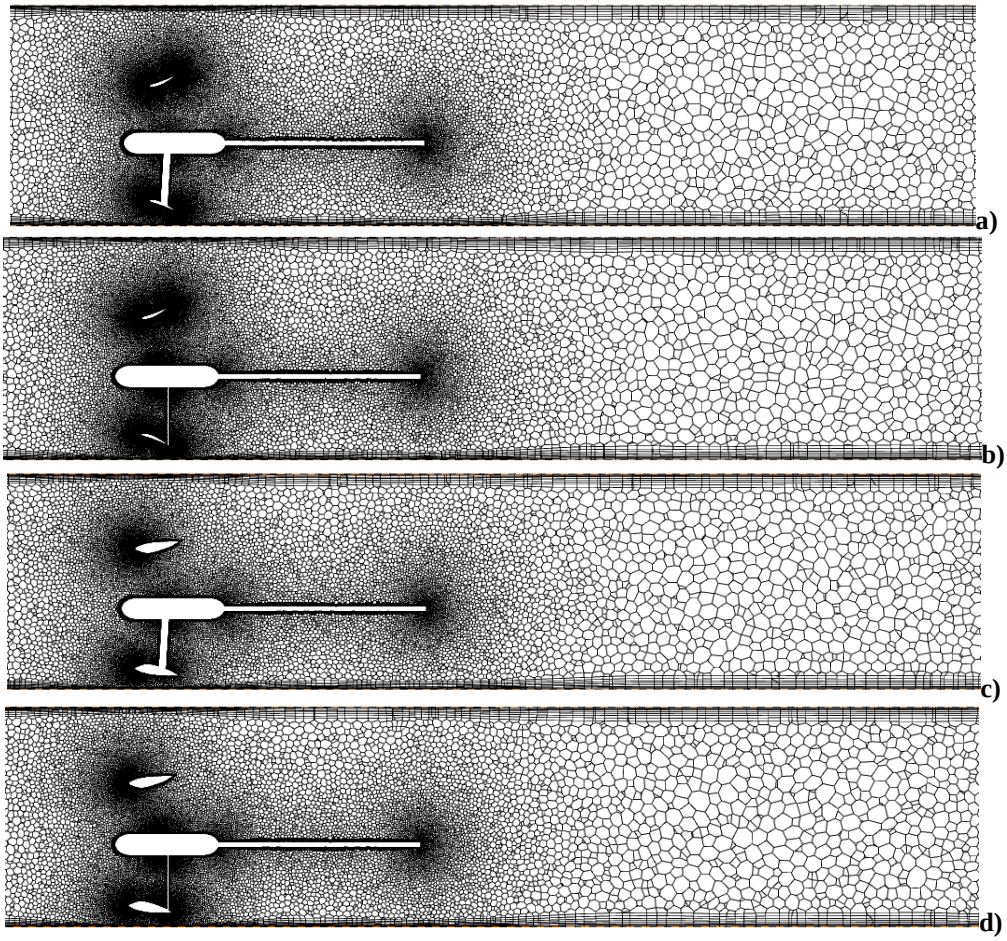

Figure 4. Mesh geometry for a) case 1, b) case 2, c) case 3, d) case 4

In the numerical domain were considered two zones one with water and one with air as shown in Figure 5. It was done like this because during the experimental measurements we observed that at the free surface of the water waves were formed. For all the studied cases was imposed a mean velocity of 0.85 m/s (Reynolds number $Re = 1.7 \cdot 10^5$) at the inlet.

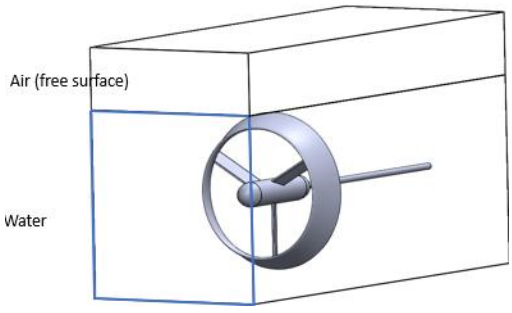

Figure 5. Schematic geometry of the numerical domain.

3. RESULTS AND DISCUSSION

In Figure 6 are presented the velocity iso-contours extracted from vertical plane in axis of shroud. In the upper part of the plane was considered the water free surface and at the bottom of the area was considered the bottom of the flow area.

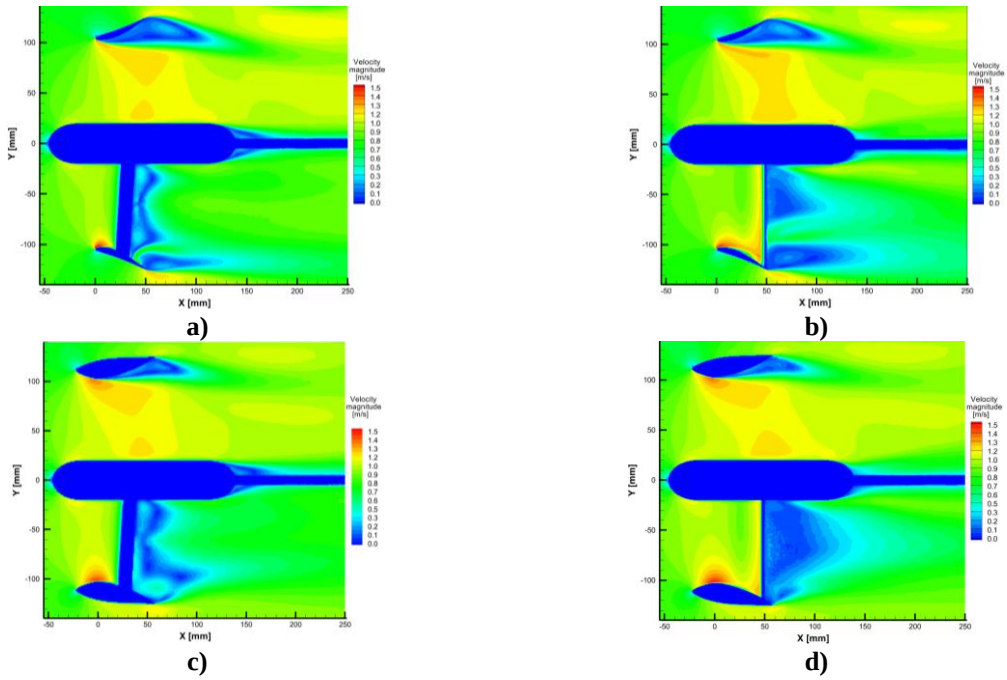

Figure 6. Velocity iso-contours extracted in median vertical plane a) case 1, b) case 2, c) case 3, d) case 4

There are some remarks to do refer to Fig. 6, one of them being the dimension of zone where the velocities decrease due to the fixing elements geometry. As can be observed in the cases with rectangular fixing elements the zones with low velocity are larger than in the case with oval fixing elements. Another remark is about the increased velocity in the area where the rotor will be placed.

The iso-contours of velocity represented in Figure 7 were extracted in shroud's axis in horizontal plane. Unlike the previous ones these are in both sides (top and bottom) were considered walls, and no fixing element is present. As in the previous figure, in Figure 7 can be observed some blues zones were the velocity decreases to 0.3 m/s. These zones are larger in cases 1 and 2 with the shroud having NACA 6142 profile. This may be due to the shroud's higher angle of inclination.

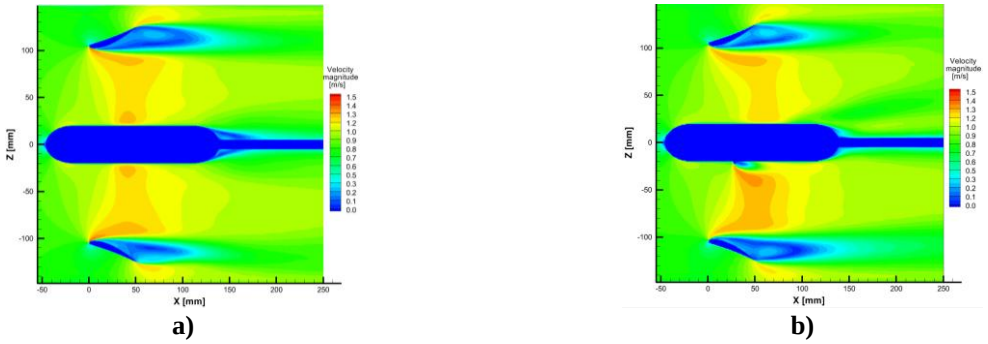

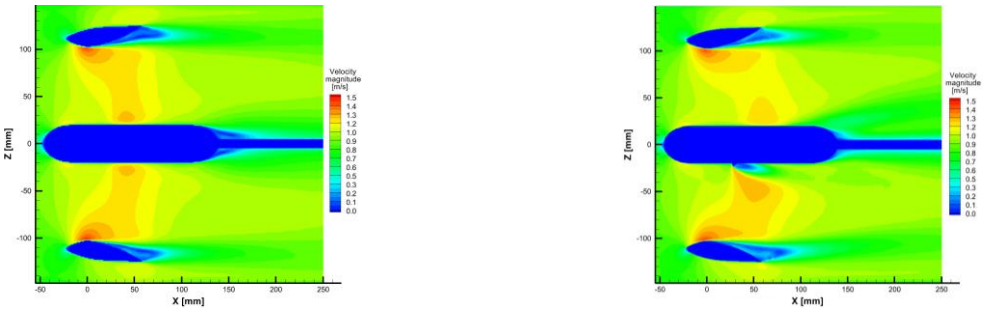

c) d)

Figure 7. Velocity iso-contours extracted in median horizontal plane a) case 1, b) case 2, c) case 3, d) case 4

Another important aspect is regarding the velocity reached in rotor zone which reach the value of 1.3 m/s for cases 1 and 2, and 1.4 m/s in cases 3 and 4. For a better visualization of the areas where the water speed increases, we extracted Figure 8 were with different colours 5 different velocity arear are represented as fallowing: dark blue zone – velocities under 1m/s; light blue zone – velocities between 1 and 1.1 m/s; green zone - velocities between 1.1 and 1.2 m/s; orange zone – velocities between 1.2 and 1.3 m/s; pink zone – velocities between 1.3 and 1.4 m/s; white zone – velocities between 1.4 and 1.5 m/s.

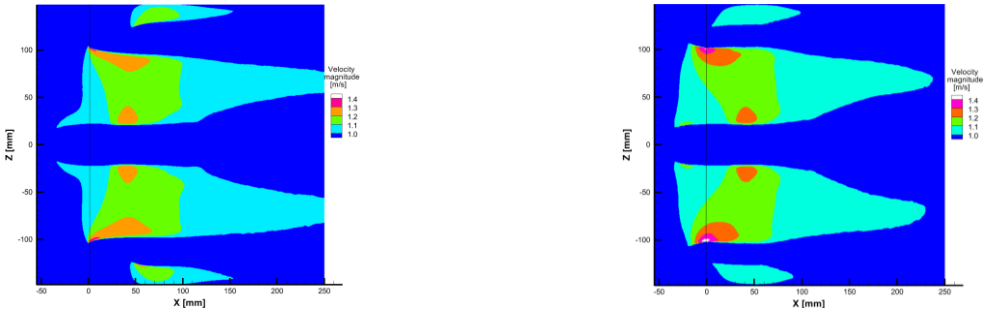

a) b)

Figure 8. Velocity iso-contours extracted in median horizontal plane a) case 1, b) case 3.

From the previous figure were extracted velocity values in the zone of rotor blades these values were represented as a graph in Figure 9. From this is clearer that the velocity inside the shrouds increases to the value of 1.45 m/s and 1.35 m/s in case of NACA profile shroud respectively convergent-divergent profile shroud. The analyzed area is the area with maximum contraction, i.e. in the section where the rotor blades will be placed. In this area maximum velocity is reached in the proximity of the shroud, respectively in the place where the tip of the rotor blades will be placed.

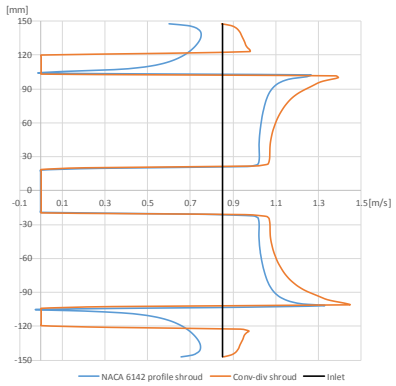

Figure 9. Velocity iso-contours extracted in median horizontal plane a) case 1, b) case 3.

The tip distance between the rotating rotor and the stationary casing leads to increased energy performance but can also induce leakage and introduce complex vortex structures. The tip-clearance size is a crucial parameter for tip-leakage vortex and considerably influences the energy performance and the operation stability of the turbine [13]. However, recommended hydrokinetic turbine blade tip clearance is a maximum of 2-3 mm. In this area, the velocity increased by 64.7%, reaching values up to 1.45 m/s.

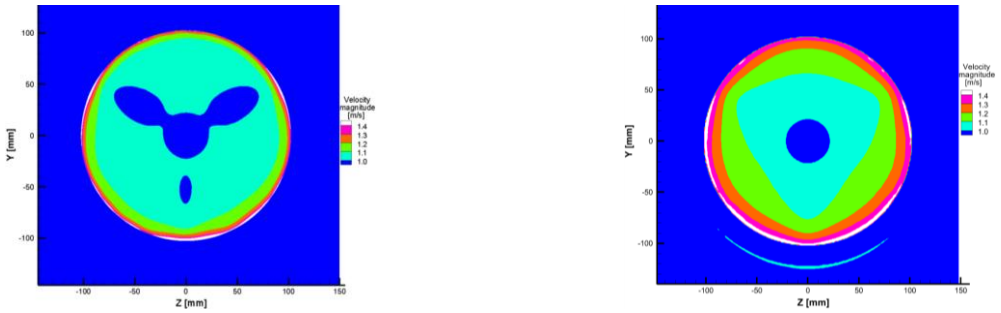

a) **b)**

Figure 10. Velocity iso-contours extracted at the face of rotor blades for a) case 1, b) case 3.

In Figure 11 are drown two curves with distances between hub and shroud in percentage and the magnitude velocity.

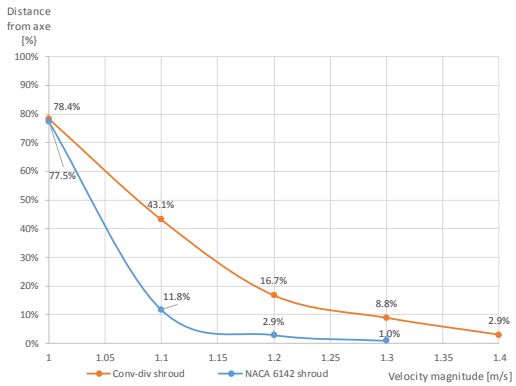

Figure 11. Curves with distances between hub and shroud in percentage and the magnitude velocity

4. CONCLUSIONS

The results presented in this study are part from a larger project which has as target to create a scaled hydrokinetic turbine. This paper presents a numerical study performed on two shroud geometries, one of these will be further implemented to the hydrokinetic turbine. For each shroud were considered two fixing elements (between shroud and hub) from the desire to install a second rotor. The numerical model used were previously validated.

The purpose of this study is to evaluate the effect of the shrouds and of the fixing element over the fluid flow velocity in the area with maximum contraction, i.e. in the section where the rotor blades will be placed. In this area maximum velocity is reached in the proximity of the shroud, respectively in the place where the tip of the rotor blades will be placed. The result shown that the new rectangular considered fixing elements did not have an influence in the fluid flow guiding and the velocity decrease in the interest area.

Regarding the shrouds effect, we found that the velocity is increased to 64.7% and 52.94% for convergent-divergent profile shroud respectively for NACA 6142 profile shroud

in the interest area. For subsequent studies we will consider convergent-divergent profile shroud and oval fixing elements.

Acknowledgment: *This paper was carried out under the subsidiary contract126-D4/2020, Hydrokinetic turbine suitable for natural and artificial watercourses, with a small head, MICROHIDRO, Transenerg, POC 2014-2020, P_40_432 / 105567, Contract no. 126/16.09.2016. The work was also supported by the Romanian Ministry of Education, Research and Digitalization, project number 25PFE/30.12.2021.*

REFERENCES

[1] Gish, L.A., Hawbaker, G., Experimental and numerical study on performance of shrouded hydrokinetic turbines, *OCEANS 2016 MTS/IEEE Monterey*, 16505939, 2016.
[2] Gaden, D.L.F., Bibeau, E.L., *Renewable Energy*, **35**(6), 1152, 2010.
[3] Scherillo, F., Maisto, U., Troise, G., Coiro, D.P., Miranda, S., Numerical and experimental analysis of a shrouded hydroturbineInternational, *Conference on Clean Electrical Power (ICCEP)*, 12291567, 2011.
[4] Limacher, E.J., Rezek, T.J., Camacho, R.G.R., Vaz, J.R.P., *Ocean Engineering*, **240**, 109940, 2021.
[5] Cardona-Mancilla, C., Sierra-Del Rio, J., Hincapie-Zuluaga, D., Chica, E., *International Journal of Renewable Energy Research*, **8**(4), 1833, 2018.
[6] Danca, P.A., Bunea, F., Nicolaie, S., Nedelcu A., Tanase, N., Babutanu, C. A., Study of hydrokinetic turbine shrouds, *10th International Conference on energy and environment (CIEM)*, 21382890, 2021.
[7] Nedelcu, A., Bunea, F., Danca, P.A., Chihaia, R.A., Babutanu, C.A., Marin, D., Ciocan, G.D., Experimental research on a hydrokinetic turbine model, *IOP Conference Series: Earth and Environmental Science*, **664**(1), 012061, 2021.
[8] Danca, P. A., Bunea, F., Babutanu, C., Nedelcu, A., Grecu, S. I., *IOP Conference Series: Earth and Environmental Science*, **1136**(1), 012058, 2023.
[9] Danca, P.A., Babutanu, C., Bunea, F., Nedelcu, A., Mixing Flow Characteristics in cylindrical tank, *IOP Conference Series: Earth and Environmental Science*, **664**(1), 012060, 2021.
[10] Sosnowski, M., Krzywanski, J., Grabowska, K., Gnatowska, R., *EPJ Web of Conferences*, **180**, 02096, 2018.
[11] Voicu, I.V., Bode, F., Abboud, W., Louahlia, H., Sandu, M., Ilinca N., *Applied Sciences*, **12**(2), 662, 2022.
[12] Salim, S.M., Ariff, M., Cheah, S.C., *Progress in Computational Fluid Dynamics, An International Journal*, **10**(5-6), 341, 2010.
[13] Liu, Y., Tan, L., Wang, B., *Energies*, **11**(9), 2202, 2018.